Applied Catalysis B: Environmental 176–177 (2015) 740–748

Contents lists available at ScienceDirect

Applied Catalysis B: Environmental

journal homepage: www.elsevier.com/locate/apcatb

Hexavalent chromium removal using metal oxide photocatalysts

Qian Cheng[a], Chengwei Wang[a], Kyle Doudrick[b], Candace K. Chan[a,*]

[a] Materials Science and Engineering, School for Engineering of Matter, Transport and Energy, 501 E Tyler Mall, ECG 301, Arizona State University, Tempe, AZ 85287, United States

[b] Department of Civil and Environmental Engineering and Earth Sciences, 156 Fitzpatrick Hall, University of Notre Dame, Notre Dame, IN 46556, United States

ARTICLE INFO

Article history:
Received 6 November 2014
Received in revised form 20 March 2015
Accepted 22 April 2015
Available online 24 April 2015

Keywords:
Hexavalent chromium
Photoreduction
Photocatalyst
Cooling tower blowdown
$NaTaO_3$

ABSTRACT

Photocatalysis is an attractive treatment method for removing hexavalent chromium (Cr(VI)) from water. Thus far, photocatalytic reduction of Cr(VI) has been investigated mostly using TiO_2 photocatalysts in acidic water solutions. Here we investigate Cr(VI) removal using zinc oxide (ZnO), tungsten trioxide (WO_3), and sodium tantalate ($NaTaO_3$), metal oxides that display good activity for other photocatalytic reactions such as water splitting, as well as titanium oxide (TiO_2, Evonik P90). The efficiency for Cr(VI) removal using these photocatalysts was investigated in synthetic neutral and alkaline water, as well as in cooling tower blowdown water. The effect of several additives used in water treatment processes on the Cr(VI) removal rate was also studied. For $NaTaO_3$, citric acid was found to have a detrimental effect to Cr(VI) removal, while sodium formate, ammonium chloride, and sodium sulfite were beneficial. While sulfite alone could chemically reduce Cr(VI), sulfite in combination with a photocatalyst resulted in faster and complete removal of Cr(VI) in 10 min using a SO_3^{2-}/Cr(VI) ratio >35 in pH ~ 8 solutions. $NaTaO_3$ was found to display the highest Cr(VI) removal rates on a photon basis at pH 3 and in the presence of sodium sulfite, while ZnO and TiO_2 showed the best performance in pH 7 and cooling tower blowdown water.

1. Introduction

Chromium is a regulated metal and abundant in ground waters as a naturally occurring metal or contaminant from industrial processes related to mining, electroplating, metal finishing, and pigments, among others [1,2]. Hexavalent chromium [Cr(VI)] compounds are carcinogenic and have been found to be anywhere from 10 to 1000 times more toxic than trivalent [Cr(III)] chromium compounds [3]. In aqueous solutions with pH 6–8, the most probable Cr(VI) species are chromate, CrO_4^{2-}, and bichromate, $HCrO_4^-$, both of which are very soluble anions that cannot form precipitates [4]. Studies have also shown that Cr(III) can become oxidized to Cr(VI) during chlorination of water [5]. For this reason, many treatment strategies have centered around reduction of Cr(VI) to Cr(III) species, which can form insoluble $Cr(OH)_3$ and be removed with adsorbents. Since Cr(VI) exists as negatively charged anion species, it can also be adsorbed onto surfaces of metal oxide sorbents if the pH of the solution is below the sorbent's point of zero charge (PZC), since the surface will be positively charged and promote electrostatic attraction. A list of PZCs, also known as isoelectric points (IEPs) for many common metal oxides and semiconductors has been compiled by Kosmulski [6].

One treatment method for removing chromium from water is to use photocatalysis. Photocatalytic degradation of harmful contaminants is becoming increasingly attractive for wastewater treatment of dilute streams, particularly with ultraviolet (UV) light emitting diodes (LEDs), which are seen as reliable, continuous, and low-cost light sources [7]. When semiconductors are irradiated with light containing photons that are more energic than the bandgap of the semiconductor, electrons are generated that can be used for reducing species. While photoexcited electrons are commonly exploited for reducing protons in water to generate hydrogen gas [8], these electrons can also be used to remove harmful contaminants for water treatment applications, such as reducing Cr(VI) to Cr(III) (Fig. 1A). In general, photocatalytic reduction is possible when the standard reduction potential of the reactant is more positive than the conduction band of the photocatalyst (Fig. 1B), although several hundred millivolts of overpotential are often required due to ohmic, kinetic, and mass transfer losses [9].

Photocatalytic reduction of Cr(VI) using photogenerated electrons from metal oxide semiconductors is attractive as a chromium treatment method, since the material can double as the

* Corresponding author. Tel.: +1 480 7278614; fax: +1 480 7279321.
E-mail address: candace.chan@asu.edu (C.K. Chan).

http://dx.doi.org/10.1016/j.apcatb.2015.04.047
0926-3373/

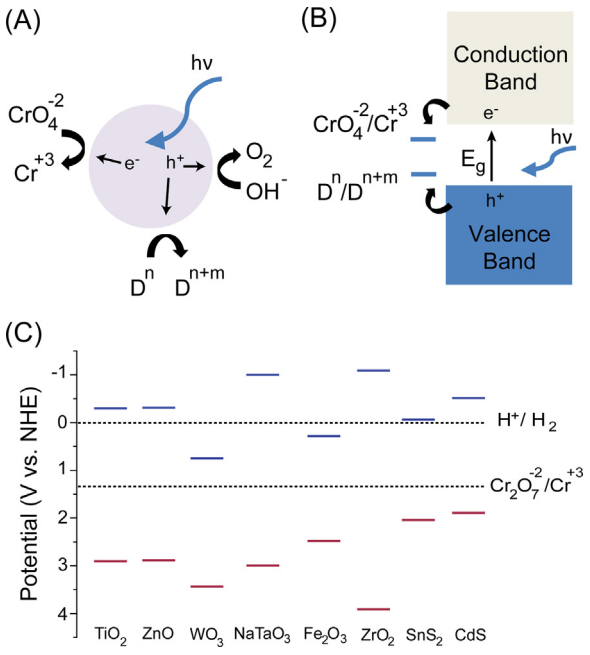

Fig. 1. (A) Schematic depicting photocatalytic reduction of hexavalent chromium (shown here as chromate) using photogenerated electrons on a semiconductor photocatalyst particle. Photogenerated holes can oxidize water or an electron donor, D^n. (B) Band diagram depiction of Cr(VI) photoreduction. The photocatalyst band edges must straddle the redox potentials for Cr(VI)/Cr^{3+} and the sacrificial reagent. (C) Band edges for common semiconductor photocatalysts at standard conditions (pH 0) with respect to the redox potentials for H_2 generation and Cr(VI)/Cr^{3+}. Conduction band edges are shown as blue lines and valence band edges in red. (For interpretation of the references to color in this figure legend, the reader is referred to the web version of this article.)

photocatalyst and adsorbent. The reduction potential of Cr(VI), which is present as dichromate ($Cr_2O_7^{2-}$) at standard conditions (e.g., pH 0), is E^0 = 1.36 V vs. RHE [10]. Most commonly studied wide bandgap semiconductors have conduction band minima [11] positive enough for the photoreduction of Cr(VI) to occur (Fig. 1C). During light irradiation, photogenerated holes are also produced, which can be used to oxidize water or a sacrificial agent, D^n (Fig. 1A). To be able to oxidize water, the valence band edge of the semiconductor must be more positive than the reduction potential for OH^-/O_2. The net reaction for Cr(VI) reduction and concurrent water oxidation in acidic and neutral environments are shown in Eqs. (1) and (2), respectively.

$$2Cr_2O_7^{2-} + 16H^+ \rightarrow 4Cr^{3+} + 8H_2O + 3O_2 \quad (1)$$

$$4CrO_4^{2-} + 20H^+ \rightarrow 4Cr^{3+} + 10H_2O + 3O_2 \quad (2)$$

From these equations, it is evident that Cr(VI) reduction is a multi-proton reduction process, making this reaction less favorable in alkaline environments. Furthermore, since most metal oxides have low PZCs, $Cr_2O_7^{2-}$ is easier to adsorb onto photocatalyst surfaces at lower pH. However, pH adjustment in real industrial applications, where there are large volumes or flow rates of water, may not be practical.

Even with suitable band edge energy, due to the slow kinetics of water oxidation, most metal oxides require an additional co-catalyst for water oxidation, such as RuO_2 or IrO_2 [12]. Due to the high cost of these precious metal co-catalysts, a more feasible approach is to exploit additives that can act as sacrificial electron donors or hole scavengers. In water treatment processes, many chemical additives that are utilized, for example to adjust pH, dechlorinate, or clean filters, may also serve as hole scavengers to promote the photoreduction of Cr(VI). At the same time, since water matrices in real water applications can be quite complex, it may also be possible for species in the water to obstruct the photocatalytic processes. Hence, it is important to evaluate photocatalysts in industrially relevant water solutions rather than solely in simulated solutions consisting of de-ionized water spiked with Cr(VI).

Here we report the evaluation of UV-absorbing photocatalysts for Cr(VI) reduction and removal in synthetic solutions as well as in water samples obtained from the Salt River Project (SRP) Santan Generating Station. The Santan facility is a natural gas powered plant with approximately 1193 MW capacity in Gilbert, AZ used to supplement base-load plants and meet peak demand. The boiler and cooling water for the Santan Generation Station are sourced from onsite wells or surface waters. Groundwater in the SRP service area contains naturally occurring levels of chromium, which can become concentrated in cooling water blowdown and hence pose challenges for meeting regulatory discharge limits. The Arizona maximum contaminant level (MCL) for Cr(VI) is 27 ppb and the NPDES regulatory discharge limit is 11 ppb [13].

The conditions required for effective Cr(VI) reduction in these waters were investigated in a labscale photocatalytic reactor. The metal oxides studied were titanium dioxide (TiO_2), zinc oxide (ZnO), tungsten trioxide (WO_3), and sodium tantalate ($NaTaO_3$). These materials were chosen because they have been well studied as photocatalysts for water splitting applications [14], and also have suitable conduction band energies for photocatalytic reduction of Cr(VI) (Fig. 1C). Of these metal oxides, TiO_2 has been the most commonly investigated photocatalyst for the reduction of Cr(VI), both in powdered slurry configurations [10] and in photoelectrochemical cells [15]. In previous studies, WO_3 displayed the highest activity for photoreduction of Cr(VI) in acidic solutions when compared to TiO_2 (both rutile and anatase crystal phases), hematite (α-Fe_2O_3), and strontium titanate ($SrTiO_3$) photoelectrodes [16]. ZnO has also been used as a photocatalyst for Cr(VI) reduction with high efficiency [17], but may not be stable when the pH is lower than 5 or higher than 10. To our knowledge, $NaTaO_3$ has not been investigated as a photocatalyst for Cr(VI) reduction. Not only does $NaTaO_3$ have a high quantum yield for overall water splitting [18], but also it can demonstrate stoichiometric H_2 and O_2 production without requiring a co-catalyst for water oxidation [19]. Hence, $NaTaO_3$ may also demonstrate promising activity for the photocatalytic reduction of Cr(VI) without the use of sacrificial hole scavengers. Table 1 summarizes the relevant properties of the photocatalysts used in this study, such as the conduction and valence band edge positions, bandgap (E_g), and PZC [6,11,20–23].

Table 1
Properties of metal oxide photocatalysts for photoreduction of Cr(VI). The conduction band minimum (CBM) and valence band maximum (VBM) are provided at pH 0. The PZC for TiO_2, ZnO, and WO_3 are reported values from the literature [6,20–22]. The PZC for $NaTaO_3$ was determined from zeta potential measurements (Fig. 2E). The usable photon flux, Φ, represents the number of photons with energies higher than E_g that could be absorbed by each material in the photoreactor.

Photocatalyst	E_g (eV)	CBM	VBM	PZC	Surface area (m^2/g)	Φ (photons/cm^2-min)
TiO_2	3.2	−0.29 V	2.91 V	5.8–6.7	92.6	7.14×10^{17}
ZnO	3.2	−0.31 V	2.89 V	8.8–9.5	7.71	7.14×10^{17}
WO_3	2.7	0.74 V	3.44 V	0.43–0.5	4.62	9.40×10^{17}
$NaTaO_3$	4	−1.00 V	3.00 V	3.5	1.57	1.55×10^{17}

2. Experimental

2.1. Materials characterization

WO_3 and ZnO were obtained from Sigma–Aldrich and used without further treatment. P90-TiO_2 was obtained from Evonik. $NaTaO_3$ was synthesized using a hydrothermal reaction as described previously [24]. In a typical synthesis, 0.44 g Ta_2O_5 and 1.2 g NaOH were added to a Teflon lined stainless-steel autoclave (Parr, 50 mL capacity) that was filled to 80% volume with DI water, heated to 140 °C for 12 h, then cooled to room temperature naturally and washed with DI water and ethanol for three times. The powder was dried in a vacuum oven for 2 h at 50 °C. X-ray diffraction (XRD, Panalytical X'pert Pro) and scanning electron microscopy (SEM, FEI XL30) were performed to determine the crystal structure and observe the morphology of the photocatalysts. The surface area of the metal oxides was determined from N_2-adsorption experiments using Brunauer–Emmett–Teller (BET) surface area analysis (Micromeritics, Tristar II).

PZC values for P90 TiO_2, ZnO, and WO_3 were obtained from published reports [6,20–22]. The PZC for $NaTaO_3$ was not available in the literature so zeta potential (ζ) measurements were performed using an electrophoretic mobility method (ZetaPALS, Brookhaven Instruments Corporation, U.S.). $NaTaO_3$ powder was added to 10 mM potassium nitrate and sonicated to create a 0.6 g/L suspension. The suspension was mixed for 24 h in the dark to achieve equilibrium with the potassium nitrate ions. Immediately before ζ analysis, the suspension was re-sonicated. A range of pH values were chosen to determine the pH PZC. The pH was adjusted using sodium hydroxide and nitric acid.

2.2. Water solutions

Simulated Cr(VI) solutions were prepared by dissolving $K_2Cr_2O_7$ in ultrapure DI water (18.3 MΩ-cm) at either 10 or 1 ppm concentrations. The pH of the solution was adjusted to 7 using NaOH and HCl. Water samples (pH 8.3) were obtained from the cooling tower blowdown at the Salt River Project Santan Generating Station, filtered to remove solids (polycarbonate filter membranes, 0.2 μm pore), and spiked with 1 ppm Cr(VI).

2.3. Photocatalytic removal of chromium

The photocatalysts were evaluated in a photoreactor composed of two borosilicate bottles (1.8 L, transmittance $\lambda > 280$ nm) submerged in a cooling tank with a medium-pressure mercury vapor lamp (450 W, Ace Glass, 7825-34) placed in a double-walled quartz immersion well (Ace Glass, 7854-25) [25]. The glass reactor (Ace Glass, 7841-05) temperature was maintained at 25 °C with a chiller. Previously, the light irradiance for the lamp in this photoreactor

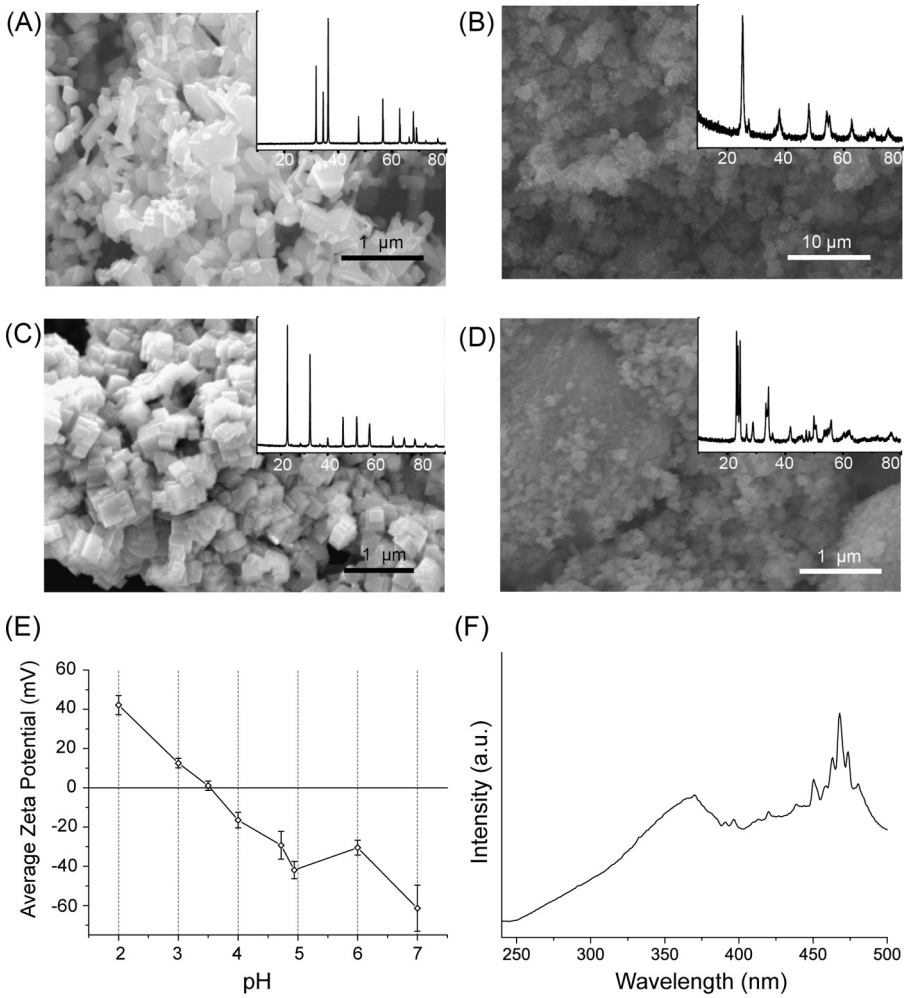

Fig. 2. SEM images of photocatalysts used. Insets show the corresponding XRD patterns. (A) ZnO, (B) TiO_2, (C) $NaTaO_3$, (D) WO_3. (E) Zeta potential analysis for $NaTaO_3$ at various pH. (F) Emission spectrum of mercury lamp used in the photoreactor.

setup was determined to be 7.66×10^{-6} Einsteins/L-s (1.654×10^{18} photons/cm^2-min) for all wavelengths 280–500 nm using ferrioxalate chemical actinometry [25]. The usable photon flux, Φ, for each photocatalyst was approximated by including only the wavelengths that could be absorbed by the photocatalyst according to its bandgap. Since only photons with energy higher than the semiconductor bandgap can be absorbed and used to excite electrons from the conduction to valence bands, Φ was calculated by integrating the number of photons with energy E_g and higher. The spectrum of the lamp is shown in Fig. 2F. The bandgaps and corresponding photon flux for each photocatalyst are listed in Table 1. The number of photons per cm^2, N, was then determined from the product of the irradiation time, t, and Φ as shown in Eq. (3).

$$N = t\Phi \tag{3}$$

To avoid direct photolysis of the organic hole scavengers, a quartz sleeve was placed around the lamp to filter out wavelengths below 285 nm. Due to the large bandgap of $NaTaO_3$ (i.e., 310 nm), Cr(VI) reduction was not observed when the quartz sleeve was used. Therefore, the quartz sleeve was removed for all $NaTaO_3$ experiments. The photocatalysts were suspended at a concentration of 1 g/L. Prior to transfer into the photoreactor, the suspension was stirred in the dark for 15 min at 700 rpm and the mercury lamp was turned on for 30 min to stabilize the light. After light irradiation, the photocatalysts were removed from the photoreactor and recovered using vacuum filtration.

2.4. Regeneration of photocatalyst

To study the ability of the photocatalyst to be reused multiple times, TiO_2 or $NaTaO_3$ were first used to reduce 10 ppm Cr(VI). After the reaction, the photocatalyst was recovered using vacuum filtration and washed with DI water for several times. Then the photocatalyst was dried at 60 °C for 2 h, and re-dispersed in 200 mL of either 1 M HNO_3 or 3 M NaOH and sonicated for 3 h. Finally, the photocatalyst was recovered with vacuum filtration, washed with DI water, then dried again for the next reuse cycle.

2.5. Analysis

The concentration of Cr(VI) remaining in the solution, which represents the amount of Cr(VI) that was not reduced or adsorbed onto the surface of the photocatalyst, was determined colorimetrically utilizing the 1,5-diphenylcarbohydrazide method in a DR-5000 UV–vis spectrometer with a TNT 854 reagent kit from Hach. Cr(III) recovered with acid or alkaline treatment of used photocatalyst was oxidized with sodium persulfate at 1 M NaOH solution by heating at 100 °C for one hour. Once the Cr(III) was oxidized to Cr(VI), it was analyzed colorimetrically as described above.

3. Results and discussion

3.1. Materials characterization

Fig. 2 shows the SEM images of the photocatalyst particles with the XRD patterns inset. The ZnO particles (Fig. 2A) were rod-shaped and ranged from 200 to 400 nm in size and adopted the hexagonal crystal structure (PDF 01-079-2205). The TiO_2 particles (Fig. 2B) had a high surface area and the crystal structure was a mixture of anatase and rutile, consistent with the specifications for P90 [25]. The $NaTaO_3$ (Fig. 2C) adopted a nanocube morphology and monoclinic crystal structure (PDF 01-074-2477). The WO_3 (Fig. 2D) was in the form of nanoparticles about 100 nm in size with monoclinic structure (PDF 00-043-1035). The surface area of the photocatalysts were determined by BET and results are listed in Table 1 with an order of $TiO_2 > WO_3 > ZnO > NaTaO_3$. This trend is expected based on the particle sizes observed in the SEM. The low surface area of $NaTaO_3$ is caused by its smooth surfaces and cubic morphology. Fig. 2E shows the ζ analysis for $NaTaO_3$ at various pH. The PZC was at approximately 3.5.

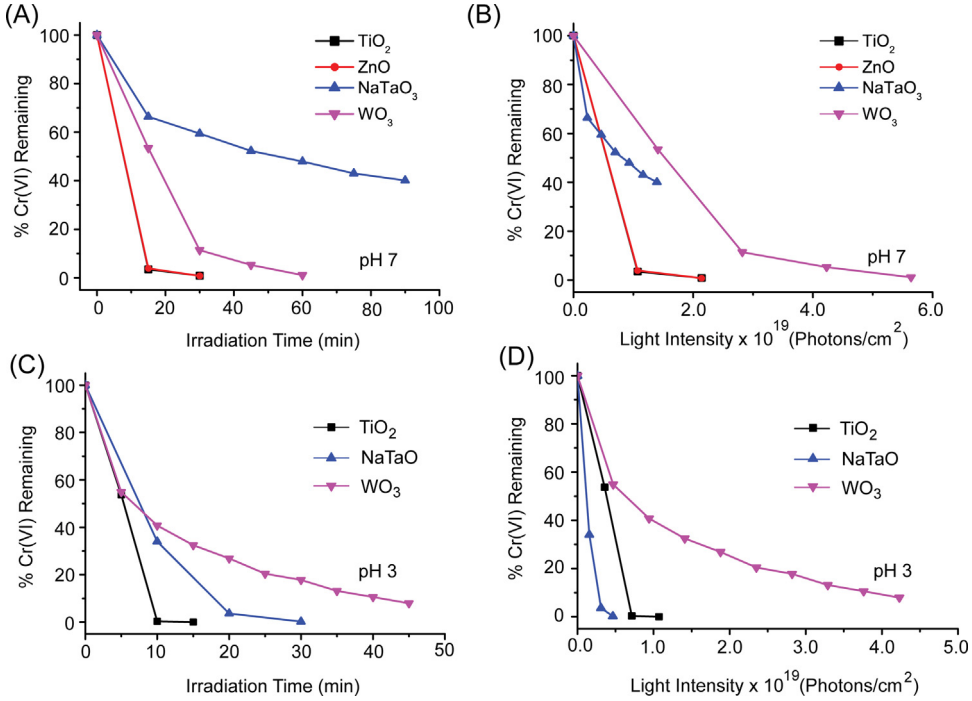

Fig. 3. Photocatalytic reduction using 1 g/L photocatalysts of (A), (B) 1 ppm Cr(VI) in DI water at pH 7 and (C), (D) 10 ppm Cr(VI) in pH 3 with formic acid. The percentage of Cr(VI) remaining is presented at different irradiation time and usable light intensity.

Table 2
Apparent kinetic constant k_{Cr} (min^{-1}) fitted from Cr(VI) reduction studies using different photocatalysts.

Photocatalyst	k_{Cr}[a]	k_{Cr}[b]	k_{Cr}[c]
TiO_2	0.1590	0.7442	0.1180
ZnO	0.1626	n/a	0.1014
WO_3	0.0824	0.0467	n/a
$NaTaO_3$	0.0068	0.2555	0.0070

[a] C_0 = 1 ppm Cr(VI); DI water, pH 7; corresponds to data in Fig. 3a.
[b] C_0 = 10 ppm Cr(VI); DI water + formic acid, pH 3; corresponds to data in Fig. 3c.
[c] C_0 = 1 ppm Cr(VI); cooling tower blowdown, pH 8.3; corresponds to data in Fig. 7a.

3.2. Cr(VI) removal in DI water

The photocatalysts were first evaluated in DI water at pH 7 spiked with 1 ppm Cr(VI). All four photocatalysts studied were found to be effective for Cr(VI) removal. Fig. 3A shows the % Cr(VI) remaining as a function of irradiation time. TiO_2 and ZnO had similar removal efficiencies and removed Cr(VI) better than WO_3 and $NaTaO_3$ at pH 7. The apparent photocatalytic reduction rate constant, k_{Cr} was achieved by fitting the Cr(VI) reduction rate to a pseudo-first-order rate reaction, as shown in Eq. (4).

$$\ln\left(\frac{C_t}{C_o}\right) = -k_{Cr}t \quad (4)$$

C_t represents the concentration of Cr(VI) at the irradiation time t and C_o is the original concentration of Cr(VI). The results, shown in the first column of Table 2, show that TiO_2 and ZnO have the highest rate constants, both around 0.16 min^{-1}, followed by WO_3 and then $NaTaO_3$. Although the PZC of TiO_2 is lower than 7, it still displayed similar Cr(VI) removal as ZnO, which has a higher PZC. The higher surface area and smaller particle size of TiO_2 could be the reason for its similar activity as ZnO at this pH. While WO_3 and $NaTaO_3$ have low PZC (3.5 for $NaTaO_3$ and 0.41 for WO_3), photoreduction of Cr(VI) was still possible at pH 7, but with lower reduction rates compared to TiO_2 and ZnO.

Fig. 3B shows the same Cr(VI) removal data, but as a function of light intensity, or photons per irradiation area (N from Eq. (3)). We point out that the light intensity here is showing the number of usable photons based on their energies with respect to the photocatalyst bandgap, without taking into consideration the number of photons that are actually absorbed and not, for instance, scattered outside the reactor without being absorbed. Photon losses due to scattering are an important factor to consider when overall photocatalytic efficiencies are concerned [26], but are highly dependent on the reactor design. In this study, the photoreactor takes advantage of inner illumination, so that the photocatalyst suspension completely surrounds the light source, and scattering is not considered. Rather, analyzing the removal rate according to the usable photon basis is performed as it is important when comparing photocatalysts with different bandgaps, since lower bandgap materials will absorb a larger portion of the light spectrum. While applications using solar light stress the importance of low bandgap (e.g., 1.1–2.0 eV) semiconductors for maximum solar energy conversion efficiency [27–29], water treatment applications using UV photocatalysis are more concerned with the treatment time and removal efficiency. In terms of removal efficiency based on the number of usable photons, $TiO_2 \sim ZnO > NaTaO_3 > WO_3$, as shown in Fig. 3B. Although WO_3 has a smaller bandgap compared to TiO_2 and ZnO, allowing it to absorb a broader range of photon energies, it still required almost three times as many photons as TiO_2 and ZnO to reach complete removal of the Cr(VI).

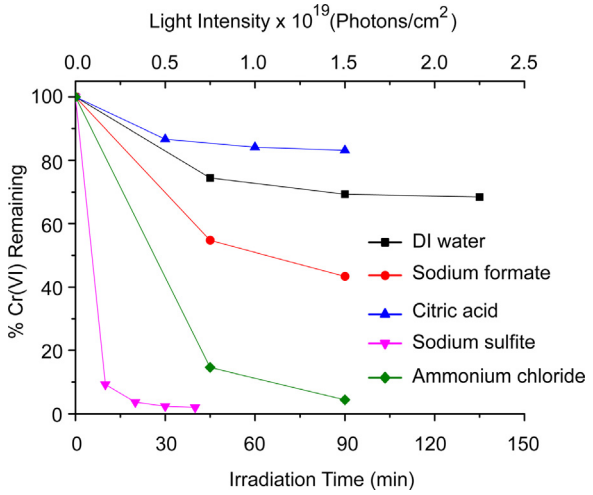

Fig. 4. Photocatalytic reduction of 10 ppm Cr(VI) using 1 g/L $NaTaO_3$ photocatalyst in DI water with and without additives. All solutions were pH 7, except for that containing Na_2SO_3, which was pH 8.45. The percentage of Cr(VI) remaining at different irradiation time (bottom axis) and usable light intensity (top axis).

The solution pH was then adjusted to 3 using excess formic acid (0.3 g/L), which can also serve as a sacrificial hole scavenger. The solution pH is an important factor in Cr(VI) reduction due to the large number of protons needed (Eqs. (1) and (2)) [30]. ZnO was not used as the photocatalyst in this case, since it could easily dissolve at this pH. The Cr(VI) removal rate greatly increased using the other three photocatalysts at pH 3 (Table 2, middle column), with all of the Cr(VI) (10 ppm initial concentration) reduced in 30 min using $NaTaO_3$ and TiO_2. Despite its higher bandgap, $NaTaO_3$ exhibited more efficient Cr(VI) removal on a photon basis than TiO_2 at pH

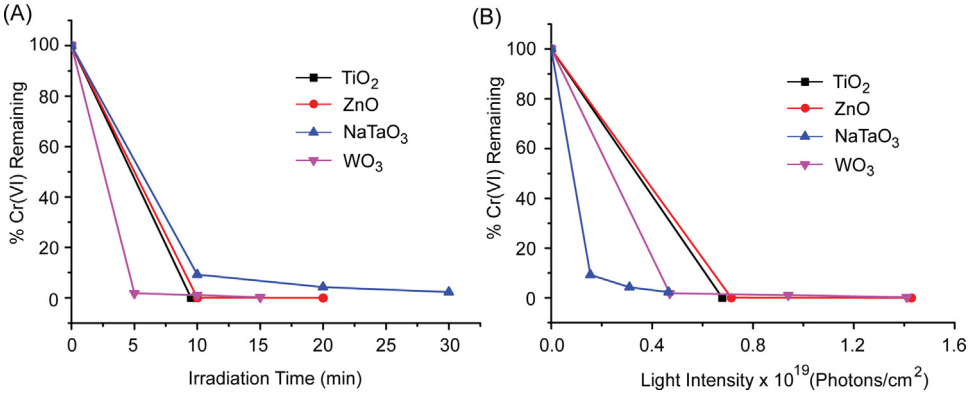

Fig. 5. Photocatalytic reduction of 10 ppm Cr(VI) using photocatalyst at 1 g/L in DI water with 0.4 g/L Na_2SO_3 at pH 8.45. The percentage of Cr(VI) remaining (A) at different irradiation time and (B) usable light intensity.

3 (Fig. 3D), which is lower than the PZC for both materials. Additionally, the $NaTaO_3$ particles had a lower surface area than TiO_2. These results suggest a higher intrinsic activity for Cr(VI) reduction on $NaTaO_3$ compared to TiO_2. The origin of this activity is not known, but possibly could be due to the much more negative conduction band edge energy in $NaTaO_3$, resulting in a higher overpotential for Cr(VI) reduction compared to TiO_2 (Fig. 1C). The Cr(VI) removal rate on WO_3 was also accelerated at pH 3 compared with pH 7, but WO_3 still needed more than eight times the photons compared with $NaTaO_3$ to achieve the same removal percentage. This can similarly be explained by the positive conduction band minimum for WO_3, giving it less overpotential for Cr(VI) reduction. The low performance of WO_3 compared to $NaTaO_3$ and TiO_2 could also be due to its low PZC value of 0.43, resulting in a negative surface charge at pH 3.

From these results, we can see that the Cr(VI) removal rate is highly dependent on different factors of the metal oxide, such as PZC, surface area, bandgap, and conduction band minimum, and cannot easily be predicted from just one of these properties.

3.3. *Effect of additives*

To better understand the effect of the water matrix on the photocatalytic removal of Cr(VI), several chemicals that are commonly used in the water treatment processes were added separately into DI water spiked with 10 ppm Cr(VI). Ammonium hydroxide is commonly used in boiler treatment as a corrosion inhibitor. Citric acid is used intermittently to clean the reverse-osmosis filters. Sodium bisulfite ($NaHSO_3$) and sodium metabisulfite ($Na_2S_2O_5$) are used as de-chlorination agents often at 1–1.3 times excess.

The results for the effect of ammonium chloride (1 g/L), citric acid (0.175 g/L), sodium sulfite (0.4 g/L), and sodium formate (0.04 g/L) on Cr(VI) removal using $NaTaO_3$ as photocatalyst are shown in Fig. 4. The addition of additives slightly changed the solution pH so it was adjusted back to 7 with either NaOH or HCl, the exception being Na_2SO_3. When using Na_2SO_3, the solution pH was maintained at 8.45, in order to better simulate the SRP cooling tower blowdown. Compared to the results where the Cr(VI) was prepared in DI water only, the addition of sodium formate, sodium sulfite, and ammonium chloride improved the rate of Cr(VI) reduction by $NaTaO_3$, whereas introduction of citric acid decreased it. These results can be explained as follows.

Ammonium can act as a good hole scavenger and enhance the Cr(VI) removal, which was previously observed with TiO_2 photocatalysts [31]. The final oxidized product of ammonium oxidation is likely nitrate, as shown in Eq. (5). During ammonium oxidation, protons are produced, which would slow down the pH increase that occurs due to proton consumption during Cr(VI) reduction, as shown in Eq. (1). This pH stabilization could also serve to enhance the Cr(VI) reduction.

$$NH_4^+ + 3H_2O \rightarrow NO_3^- + 8e^- + 10H^+ \quad (5)$$

Similar to formic acid, adding citric acid to the water decreased the pH to 3, which enhanced the photoreduction reaction and decreased the Cr(VI) concentration by >98% after 90 min (not shown). However, when NaOH was added along with the citric acid to maintain a neutral solution pH, the Cr(VI) removal on $NaTaO_3$ was markedly decreased compared to the additive-free DI water solutions (Fig. 4). These results show that at neutral pH, citric acid does not act as a hole scavenger to enhance Cr(VI) reduction. This could be due to the fact that the tertiary hydroxyl and three carbonyl groups make oxidation of citric acid more difficult compared to other organic acids [32]. Moreover, at pH 7, citric acid is completely deprotonated ($pKa_3 = 6.40$) with three negatively charged carboxylic acid groups. At this pH, the surface of $NaTaO_3$ is negatively charged, which would make it difficult for citrate ions to adsorb onto the surface.

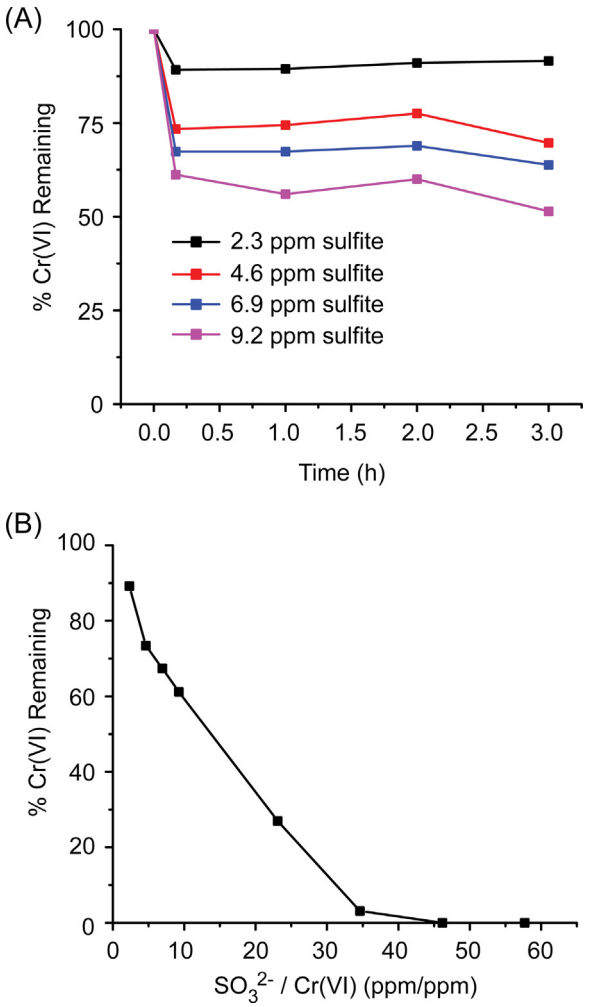

Fig. 6. (A) Chemical reduction of 1 ppm Cr(VI) using varying amounts of Na_2SO_3, (B) Percent of Cr(VI) remaining after chemical reduction by Na_2SO_3 as a function of different sulfite to Cr(VI) ratios.

As shown in Fig. 4, the presence of sulfite resulted in the fastest Cr(VI) removal on $NaTaO_3$. A series of experiments was conducted to determine the optimum amount needed. These studies were first performed using all the photocatalysts and the results are shown in Fig. 5. When using 0.4 g/L sodium sulfite with TiO_2, ZnO, and WO_3, all of the Cr(VI) (10 ppm starting concentration) was removed within 15 min (Fig. 5A). The Cr(VI) removal on $NaTaO_3$ was slower on the time scale due to its larger bandgap, but it was the most efficient when considering the photon basis (Fig. 5B).

Sodium sulfite, bisulfite, and metabisulfate have been shown to act as very effective chemical reductants of Cr(VI), with fast and complete reduction at pH 2–5 [33]. The reduction reaction with sulfite is shown in Eq. (6).

$$2CrO_4^{2-} + 3SO_3^{2-} + 10H^+ \rightarrow 2Cr^{3+} + 3SO_4^{2-} + 5H_2O \quad (6)$$

However, the pH of the SRP waters usually ranges from 7.6 to 8.6 and it is not clear how effective sulfite would be for chemical reduction of Cr(VI) at these pH values. Therefore, control tests were performed wherein sodium sulfite alone was added to the Cr(VI) solutions to better understand the chemical reduction in the pH range 8.45–8.85. At low SO_3^{2-}/Cr(VI), the reduction reaction was fast, but only partial Cr(VI) reduction was observed. Fig. 6 shows the effect of increasing amounts of sodium sulfite in solutions

Table 3
Regeneration of TiO_2 photocatalyst with acid or alkaline treatment. M_{Cr1} is the mass of Cr(VI) that was removed from the photoreduction and deposited on the surface of TiO_2 (0.2 g) after irradiation for 45 min in DI water at pH 7. M_{Cr2} is the mass of Cr(III) leached in the alkaline or acid treatment.

Regeneration condition	M_{Cr1} (mg)	M_{Cr2} (mg)
3 M NaOH	2	1.122
1 M HNO_3	2	0.346

containing 1 ppm Cr(VI). For each sulfite dose, the reduction was observed to occur within 10 min and the Cr(VI) concentration remained relatively constant after that. According to Eq. (6), 1.5 moles of sulfite are required to completely reduce 1 mol of Cr(VI), which is equivalent to 2.3 ppm sulfite for 1 ppm Cr(VI). However, as shown in Fig. 6A, 2.3 ppm sulfite was only able to reduce about 10% of the Cr(VI). Even when increasing the sulfite concentration to 9.2 ppm (4× excess), only about 40% of the Cr(VI) could be removed.

To better understand the dosage requirements needed for complete sulfite reduction of Cr(VI), a series of different SO_3^{2-}/Cr(VI) ratios (ppm/ppm) were prepared. The percentage of Cr(VI) remaining after 10 min was determined. As shown in Fig. 6B, the Cr(VI) could be completely removed for SO_3^{2-}/Cr(VI) >35 within 10 min. These results highlight the need for excess sulfite in order to have effective and fast chemical reduction of Cr(VI) at pH > 8.

Comparing these results to those in Fig. 5 where SO_3^{2-}/Cr(VI) = 25, it is apparent that the presence of the photocatalyst improves the rate of Cr(VI) reduction, since this amount of sodium sulfite alone was not sufficient to remove all of the Cr(VI) in 10 min. Hence, use of both photocatalyst and sodium sulfite can reduce the Cr(VI) more quickly and with less sulfite required compared to use of sulfite alone as a chemical reductant. In the presence of photocatalyst, the sulfite is oxidized by the photogenerated holes rather than the Cr(VI). The standard reduction potential for the sulfate/sulfite redox reaction is $E^0 = -0.936$ V vs. NHE, making the potential difference (i.e., thermodynamic driving force) between sulfite and the energy of a hole in the valence band of a metal oxide semiconductor (Fig. 1C) much larger than the potential difference between sulfite and Cr(VI). The kinetics of the sulfite oxidation with photogenerated holes may also be faster than the sulfite oxidation by Cr(VI). Thus, residual sulfite in the water matrix will be beneficial for Cr(VI) removal via photocatalytic reduction.

3.4. Cr(VI) removal in cooling tower blowdown

Industrial water matrices can be quite complex, making treatment more difficult than in DI water. For example, metal levels in cooling tower blowdown can be increased multiple times that found in the makeup water due to repeated cycles of concentration. Blowdown can also contain high levels of total dissolved solids (TDS) >2000 ppm and anions such as sulfate and nitrate than can affect sorption-based treatment methods [34], as well as act as electron scavengers [25,35,36]. For example, average total chromium levels at the Santan Generating Station measured in December 2012–January 2013 increased from 5.4 ppb in the influent makeup water to 18 ppb in the cooling tower blowdown, with most of the total chromium in the hexavalent form due to oxidative conditions in the water treatment process [37].

The TiO_2, ZnO, and $NaTaO_3$ photocatalysts were evaluated in cooling tower blowdown water obtained from the Santan facility. The pH of the water was 8.3 and 1 ppm of Cr(VI) was added due to the low natural concentration of chromium. As shown in Fig. 7, the Cr(VI) removal in the blowdown was very similar to that observed in DI water (Fig. 3A and B). The apparent photocatalytic reduction rate constant k_{Cr} is also shown in the right column of Table 2. The slightly lower reduction velocity compared to the DI water at pH 7 is likely due to the higher concentration of competing anions and impurities in the blowdown. When using TiO_2 and ZnO, 30 min of irradiation was sufficient to completely remove the Cr(VI). Similar as in the pH 7 DI water, the $NaTaO_3$ displayed the slowest Cr(VI) reduction. Because sulfite-based dechlorination agents are used in excess in the facility, there may be sulfite ion residual in the blowdown water. However, the concentration of sulfite did not appear to be high enough to lead to significant improvement of the Cr(VI) removal using $NaTaO_3$ in the blowdown compared to pH 7 DI water.

3.5. Regeneration experiments on used photocatalyst

Another important aspect to consider is the ability for the photocatalyst to be regenerated and reused after Cr(VI) removal. Trivalent chromium species can form insoluble $Cr(OH)_3$ and precipitate in solution when the pH is higher than 5.5 [38]. When Cr(III) is formed via photoreduction, it can be adsorbed on the surface of the photocatalyst [39]. For an initial Cr(VI) concentration of 5 ppm, the $Cr(OH)_3$ deposited onto TiO_2 photocatalyst was distinguished by its green color [39]. In our experiments using a 10 ppm initial Cr(VI) concentration, the used photocatalysts turned green after filtration and washing, indicating that Cr(VI) was successfully reduced by the photocatalyst and removed from the system in the form of $Cr(OH)_3$.

However, the precipitated Cr(III) may inhibit further Cr(VI) reduction by occupying the reaction sites on photocatalyst and blocking the incident photons [38]. This type of photocatalyst poisoning has been observed before, especially for large initial concentrations of Cr(VI) [39,40]. Since $Cr(OH)_3$ is an amphoteric

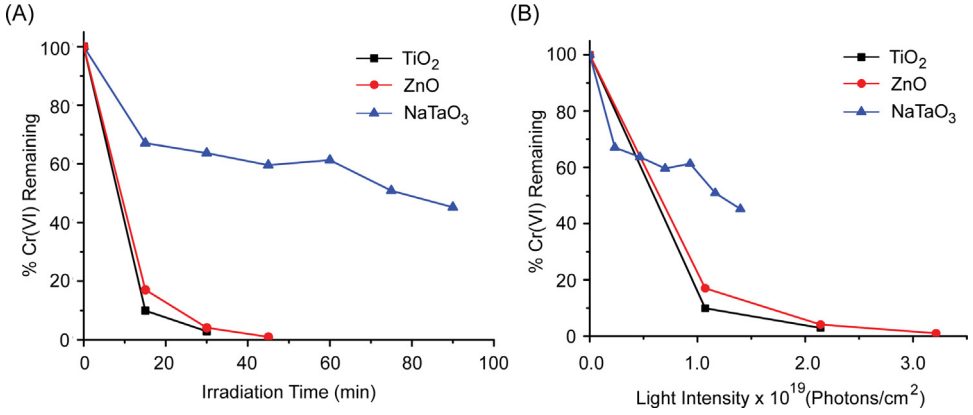

Fig. 7. Photocatalytic reduction of 1 ppm Cr(VI) using photocatalyst at 1 g/L in cooling tower blowdown water with pH 8.3. The percentage of Cr(VI) remaining (A) at different irradiation time and (B) usable light intensity.

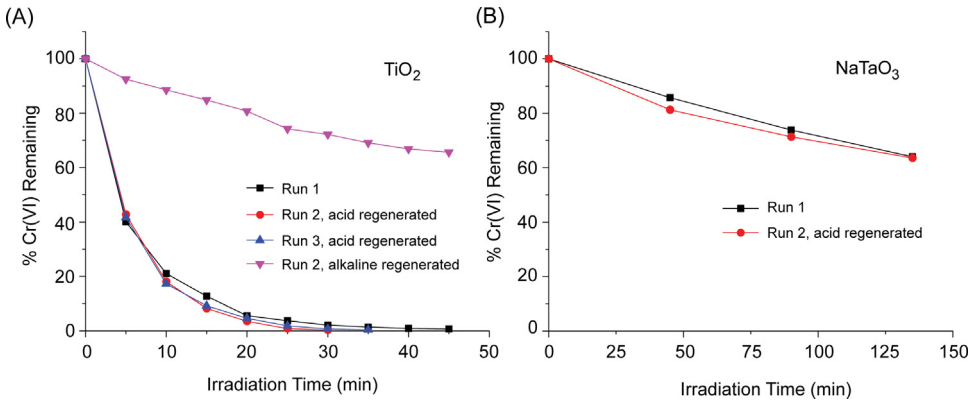

Fig. 8. Removal of 10 ppm Cr(VI) in DI water at pH 7 on pristine and regenerated photocatalysts (A) TiO_2 and (B) $NaTaO_3$.

hydroxide, it can react with either acids or bases, and thus there are different protocols in the literature for regenerating used photocatalysts [39]. Both nitric acid and sodium hydroxide were investigated as regenerating solutions for TiO_2 after it had been used to reduce 10 ppm Cr(VI). The amount of Cr(VI) removed, assuming that all species removed from solution was adsorbed onto the photocatalyst, is shown in the first column of Table 3. Surprisingly the TiO_2 photocatalyst after the treatment still looked light green in color, with the acid treated TiO_2 greener than the alkaline treated one. This suggests that there was a certain amount of Cr(III) left on the surface, and that the acid treatment was less effective than the alkaline one to remove the $Cr(OH)_3$. The leachate consisting of the regeneration solution was analyzed for Cr(VI) and Cr(III). No Cr(VI) was observed as expected, since there were no oxidizers present. The amount of Cr(III) in the leachate is shown in the second column of Table 3. These results show that about 44% of the Cr(III) remained adsorbed on the TiO_2 after the alkaline treatment, whereas almost 83% remained when treated with acid.

To examine the effect of regeneration, the acid or alkaline treated TiO_2 was used to photocatalytically reduce another DI water solution containing 10 ppm Cr(VI). These results are shown in Fig. 8a (Run 2). Despite the presence of residual Cr(III) on the surface, the removal rate for the acid regenerated TiO_2 was similar as the Run 1 using pristine TiO_2. Since the TiO_2 has a higher surface area (92.6 m^2/g), it is possible that there are still enough reaction sites available for further Cr(VI) reduction. The TiO_2 regenerated in NaOH, however, showed poorer photoreduction rates. This difference could be explained by a change in surface properties as a result of the acid and alkaline treatments. When TiO_2 is treated with acid, the surface becomes protonated and dichromate can more easily bind the surface, as shown in Eq. (7): [39].

$$TiOH_2^+ + Cr_2O_7^{2-} \rightarrow TiOH - Cr_2O_7^{2-} + H^+ \quad (7)$$

When treated with NaOH, the surface of TiO_2 is covered with hydroxyl groups and would be neutral or negatively charged, which would prevent the surface from adsorbing chromate ions.

Table 4
Apparent rate constant fitted from reaction of bare and regenerated photocatalyst based on pseudo-first-order equation.

Photocatalyst	Run	k_{Cr} (min^{-1})
TiO_2	Run 1	0.1102
	Run 2, acid regenerated	0.1886
	Run 3, acid regenerated	0.1585
	Run 2, alkaline regenerated	0.0095
$NaTaO_3$	Run 1	0.0033
	Run 2, acid regenerated	0.0033

Based on these results, only nitric acid was used to regenerate $NaTaO_3$. The Cr(VI) removal for the first and second (e.g., regenerated) runs are shown Fig. 8b. All of the apparent rate constants are listed in Table 4 for comparison. Similar to the TiO_2 case, the acid regenerated $NaTaO_3$ showed similar Cr(VI) removal properties as the pristine $NaTaO_3$. These results show that both $NaTaO_3$ and TiO_2 could be stable during regeneration and recover their activity with acid treatment.

4. Conclusions

TiO_2, ZnO, WO_3, and $NaTaO_3$ were investigated as photocatalysts for Cr(VI) removal. All four photocatalysts were found to be effective for Cr(VI) photoreduction, but the removal rates are affected by characteristics of the material (surface area, bandgap, PZC, conduction band minimum) as well as properties of the water matrix. In DI water at pH 7, the order of removal efficiency from high to low was: $TiO_2 \sim ZnO > NaTaO_3 > WO_3$. When the pH was adjusted to 3, $NaTaO_3$ exhibited high Cr(VI) removal efficiency, and the order changed to $NaTaO_3 > TiO_2 > WO_3$ with ZnO unstable at this pH. A few common industrial additives were examined and the improvement on Cr(VI) removal using $NaTaO_3$ from high to low was: sodium sulfite > ammonium chloride > sodium formate. At neutral pH, citric acid was found to inhibit Cr(VI) reduction with $NaTaO_3$. Sulfite alone could remove Cr(VI) by chemical reduction, but required large quantities in excess. The combination of sulfite and photocatalyst greatly improved the Cr(VI) removal. Cr(VI) removal using photocatalysts was only slightly affected by other constituents in cooling tower blowdown and had similar removal rates as those observed in pH 7 DI water. Different regeneration protocols were applied to the used photocatalysts. The alkaline treatment was more effective for removing adsorbed Cr(III) compared to nitric acid treatment, but acid treated TiO_2 had better subsequent Cr(VI) reduction capabilities due to surface modifications that enhanced Cr(VI) adsorption. Both acid regenerated TiO_2 and $NaTaO_3$ demonstrated comparable Cr(VI) reduction rates with the pristine forms, indicating that these photocatalysts could be stable during regeneration and recycled for multiple uses. These results show that large scale wastewater treatment using metal oxide photocatalysts to remove Cr(VI) may be possible.

Acknowledgements

This work was funded through the Arizona State University/Salt River Project Joint Research Program, under the project "Hexavalent chromium, selenium and arsenic occurrence, fate and treatment in powerplant discharge, canals, and potable water treatment plants". We would like to thank Paul Westerhoff, Allie Bowen,

and Peter Fox for fruitful and stimulating discussion. We would also like to thank Donald Pelley, Fredrick Fuller, Robert Olsen, and Gregg Elliot from Salt River Project for their support of this research.

References

[1] D. Mohan, C.U. Pittman Jr., J. Hazard. Mater. 137 (2006) 762–811.
[2] J.J. Testa, M.A. Grela, M.I. Litter, Environ. Sci. Technol. 38 (2004) 1589–1594.
[3] S.A. Katz, H. Salem, J. Appl. Toxicol. 13 (1993) 217–224.
[4] C.E. Barrera-Díaz, V. Lugo-Lugo, B. Bilyeu, J. Hazard. Mater. 223 (2012) 1–12.
[5] D.R. Lindsay, K.J. Farley, R.F. Carbonaro, J. Environ. Monitor. 14 (2012) 1789–1797.
[6] M. Kosmulski, J. Colloid Interface Sci. 253 (2002) 77–87.
[7] M. Izadifard, G. Achari, C.H. Langford, Catalysts 3 (2013) 726–743.
[8] A. Kudo, Y. Miseki, Chem. Soc. Rev. 38 (2009) 253–278.
[9] M.F. Weber, M.J. Dignam, J. Electrochem. Soc. 131 (1984) 1258–1265.
[10] W. Lin, C. Wei, K. Rajeshwar, J. Electrochem. Soc. 140 (1993) 2477–2482.
[11] Y. Xu, M.A. Schoonen, Am. Mineral. 85 (2000) 543–556.
[12] M.I. Litter, Adv. Chem. Eng. 36 (2009) 37–67.
[13] J.C. Farmer, S.M. Bahowick, J.E. Harrar, D.V. Fix, R.E. Martinelli, A.K. Vu, K.L. Carroll, Energy Fuels 11 (1997) 337–347.
[14] A. Fujishima, K. Honda, Nature 238 (1972) 37–38.
[15] Q. Wang, J. Shang, T. Zhu, F. Zhao, J. Mol. Catal. A: Chem. 335 (2011) 242–247.
[16] H. Yoneyama, Y. Yamashita, H. Tamura, Nature 282 (1979) 817–818.
[17] J. Doménech, J. Muñoz, Electrochim. Acta 32 (1987) 1383–1386.
[18] H. Kato, K. Asakura, A. Kudo, J. Am. Chem. Soc. 125 (2003) 3082–3089.
[19] H. Tüysüz, C.K. Chan, Nano Energy 2 (2013) 116–123.
[20] M. Kosmulski, J. Colloid Interface Sci. 298 (2006) 730–741.
[21] G.A. Parks, P.D. Bruyn, J. Phys. Chem. 66 (1962) 967–973.
[22] R.H. Yoon, T. Salman, G. Donnay, J. Colloid Interface Sci. 70 (1979) 483–493.
[23] Y. Deng, Y. Chen, B. Chen, J. Ma, J. Alloys Compd. 559 (2013) 116–122.
[24] X. Li, J. Zang, J. Phys. Chem. C 113 (2009) 19411–19418.
[25] K. Doudrick, O. Monzón, A. Mangonon, K. Hristovski, P. Westerhoff, J. Environ. Eng. 138 (2012) 852–861.
[26] A. Manassero, M.L. Satuf, O.M. Alfano, Chem. Eng. J. 225 (2013) 378–386.
[27] L.C. Seitz, Z. Chen, A.J. Forman, B.A. Pinaud, J.D. Benck, T.F. Jaramillo, ChemSusChem 7 (2014) 1372–1385.
[28] R.E. Rocheleau, E.L. Miller, Int. J. Hydrogen Energy 22 (1997) 771–782.
[29] W. Shockley, H.J. Queisser, J. Appl. Phys. 32 (1961) 510–519.
[30] N. Daneshvar, D. Salari, S. Aber, J. Hazard. Mater. 94 (2002) 49–61.
[31] C. Chenthamarakshan, K. Rajeshwar, E.J. Wolfrum, Langmuir 16 (2000) 2715–2721.
[32] K. Hartani, Z. Khan, Transition Met. Chem. 25 (2000) 478–484.
[33] J. Beukes, J. Pienaar, G. Lachmann, E. Giesekke, Water SA 25 (1999) 363–370.
[34] S. Kaliappan, C. Sathish, T. Nirmalkumar, J. Ind. Inst. Sci. 85 (2013) 215.
[35] T. Yang, K. Doudrick, P. Westerhoff, Water Res. 47 (2013) 1299–1307.
[36] K. Doudrick, T. Yang, K. Hristovski, P. Westerhoff, Appl. Catal. B 136 (2013) 40–47.
[37] A. Bowen, Occurrence and Treatment of Hexavalent Chromium and Arsenic in Arizona Municipal and Industrial Waters, M.S., Dissertation, Arizona State University, 2014.
[38] J.A. Navıío, G. Colon, M. Trillas, J. Peral, X. Domenech, J.J. Testa, J. Padron, D. Rodrıíguez, M.I. Litter, Appl. Catal. B 16 (1998) 187–196.
[39] S. Tuprakay, W. Liengcharernsit, J. Hazard. Mater. 124 (2005) 53–58.
[40] W. Liu, J. Ni, X. Yin, Water Res. 53 (2014) 12–25.